JBC RESEARCH ARTICLE

# Alkaline-sensitive two-pore domain potassium channels form functional heteromers in pancreatic β-cells

Received for publication, November 8, 2021, and in revised form, August 26, 2022 Published, Papers in Press, September 5, 2022,
https://doi.org/10.1016/j.jbc.2022.102447

**Lamyaa Khoubza[1,‡], Nicolas Gilbert[1,‡], Eun-Jin Kim[2], Franck C. Chatelain[1], Sylvain Feliciangeli[1,3], Sophie Abelanet[1], Dawon Kang[2], Florian Lesage[1,3,*], and Delphine Bichet[1]**

*From the [1]Université côte d'Azur, IPMC CNRS UMR7275, Laboratory of Excellence ICST, Valbonne, France; [2]Department of Physiology, College of Medicine and Institute of Health Sciences, Gyeongsang National University, Jinju, South Korea; [3]Inserm, Paris, France*

Edited by Mike Shipston

**Two-pore domain $K^+$ channels ($K_{2P}$ channels), active as dimers, produce inhibitory currents regulated by a variety of stimuli. Among them, TWIK1-related alkalinization-activated $K^+$ channel 1 (TALK1), TWIK1-related alkalinization-activated $K^+$ channel 2 (TALK2), and TWIK1-related acid-sensitive $K^+$ channel 2 (TASK2) form a subfamily of structurally related $K_{2P}$ channels stimulated by extracellular alkalosis. The human genes encoding these proteins are clustered at chromosomal region 6p21 and coexpressed in multiple tissues, including the pancreas. The question whether these channels form functional heteromers remained open. By analyzing single-cell transcriptomic data, we show that these channels are coexpressed in insulin-secreting pancreatic β-cells. Using *in situ* proximity ligation assay and electrophysiology, we show that they form functional heterodimers both upon heterologous expression and under native conditions in human pancreatic β-cells. We demonstrate that heteromerization of TALK2 with TALK1 or with TASK2 endows TALK2 with sensitivity to extracellular alkalosis in the physiological range. We further show that the association of TASK2 with TALK1 and TALK2 increases their unitary conductance. These results provide a new example of heteromerization in the $K_{2P}$ channel family expanding the range of the potential physiological and pathophysiological roles of TALK1/TALK2/TASK2 channels, not only in insulin-secreting cells but also in the many other tissues in which they are coexpressed.**

Two-pore domain $K^+$ channels ($K_{2P}$ channels) produce inhibitory background potassium currents regulated by a variety of chemical and physical stimuli (1–3). They are active as dimers of subunits, with each subunit containing four membrane-spanning segments (M1 to M4) and two pore domains (P1 and P2). Their N and C termini are intracellular. The TWIK1-related alkalinization-activated $K^+$ channel 1 (TALK1), TWIK1-related alkalinization-activated $K^+$ channel 2 (TALK2), and TWIK1-related acid-sensitive $K^+$ channel 2 (TASK2) form a subgroup of structurally and functionally related $K_{2P}$ channels (Fig. 1*A*). TALK1 shares 44% sequence identity with TALK2 and 39% with TASK2, whereas TALK2 and TASK2 share 37% sequence identity (4, 5) (Fig. 1*A*). They produce $K^+$ currents that share the particularity to be stimulated by alkalinization of the extracellular medium (4–6). They are also activated by nitric oxide and reactive oxygen species and intracellular pH (6). Recent research suggests a regulatory function of TALK1 for glucose-dependent β-cell second-phase insulin and δ-cell somatostatin secretion (7, 8). The role of TALK1 in glucose-stimulated insulin secretion (GSIS) is further supported by the fact that islet β-cells from TALK1 KO mice exhibit increased $V_m$ depolarization, augmented $Ca^{2+}$ influx, and elevated second phase GSIS (7). In human, the TALK1 polymorphism rs1535500, which results in a gain of function (A277E), has been linked to an increased risk of type 2 diabetes (9, 10). More recently, another gain-of-function mutation in TALK1 (L114P) was identified in a family with maturity-onset diabetes of the young. Both mutations resulted in reduced GSIS because of impaired intracellular $Ca^{2+}$ homeostasis (7, 11). Very little is known about the physiological function of TALK2, as this channel is absent in mice. A gain-of-function mutation in TALK2 (G88R) was described in a human patient with another mutation in a sodium channel gene (*SCNA5*) with a cardiac phenotype suggesting that TALK2 may act as a modifier of cardiac arrhythmia (12). In contrast to TALK2, TASK2 channel has been implicated in several functions mostly in brain and kidneys. TASK2 is involved in central oxygen chemoreception (13), cell volume regulation, and bicarbonate reabsorption in the kidney (14, 15). A loss-of-function mutation (T180P) with dominant-negative (DN)effect on wildtype TASK2 has been reported with higher frequency among patients predisposed to Balkan endemic nephropathy, a chronic kidney disease (16, 17).

Heterodimerization between pore-forming subunits occurs within the $K_{2P}$ channel family (see Ref. (18) for recent review). Heterodimeric channels often exhibit unique electrophysiological and pharmacological properties compared with the corresponding homodimers. By mixing and matching subunits, heteromerization increases functional diversity and contributes to pharmacological heterogeneity in the $K_{2P}$ channel family. The first demonstration of heteromerization

‡ These authors contributed equally to this work.
* For correspondence: Florian Lesage, lesage@ipmc.cnrs.fr.

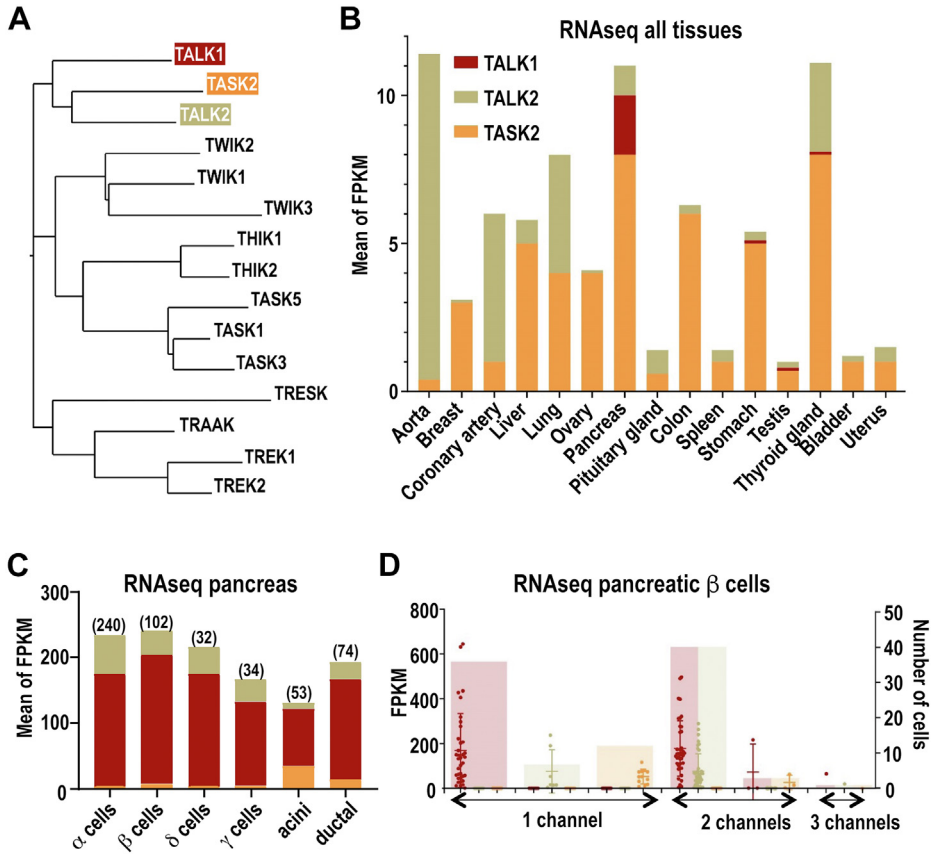


**Figure 1. Expression pattern of TALK1, TALK2, and TASK2 channels from RNA-Seq database analysis.** *A*, TALK1, TALK2, and TASK2 position within the $K_{2P}$ phylogenetic tree of human $K_{2P}$ channels. *B*, human tissue distribution. Expression levels are expressed as the mean of fragments per kilobase of transcript, per million mapped reads (FPKM). mRNA-Seq datasets were extracted from the EMBL database in a study of 1641 samples across 43 tissues from 175 individuals (GTEx consortium). *C*, expression levels in various human pancreatic cell population, including α, β, γ, ε acinar, and ductal cells. Single-cell transcriptomic data were from 2209 cells. The number of cells analyzed for each population is indicated. *D*, expression in individual human β-cells. Cells are divided into three groups displaying cells expressing a unique TALK/TASK subunit (one channel), two subunits (two channels), and three subunits (three channels). GTEx, Genotype-Tissue Expression; $K^{2P}$, two-pore domain potassium; TALK1, TWIK1-related alkalinization-activated $K^+$ channel 1; TALK2, TWIK1-related alkalinization-activated $K^+$ channel 2; TASK2, TWIK1-related acid-sensitive $K^+$ channel 2.

was between TASK1 and TASK3 (19). Then the following heterodimers were reported: THIK1/THIK2, TREK1/TREK2, TREK1/TRAAK, and TREK2/TRAAK (20–23). Heterodimers between members of different subgroups of $K_{2P}$ channels have also been described: TWIK1/TASK1 or 3, TWIK1/TREK1 or 2, TASK1/TALK2, and TRESK/TREK1,2 (24–29). Although some of these intergroup heterodimers have been confirmed by independent studies, others remain unclear as they were not detected by other studies (18).

The genes encoding TALK1 (*KCNK16*), TALK2 (*KCNK17*), and TASK2 (*KCNK5*) are located in the same chromosomal region (6p21), *KCNK16* being separated from *KCNK17* by less than 1 kb (4). This genetic clustering suggests that their transcription may be coordinated (at least partially), and that these channel subunits may associate to form heterodimeric channels. TALK1 is expressed in pancreatic cells and gastric somatostatin cells (6, 8). Low signal expression was also detected in the small intestine and stomach (30). TALK1, TALK2, and TASK2 are all expressed in the pancreas. Unlike TALK1, TALK2 and TASK2 are expressed in other tissues. TALK2 is present in placenta, lung, liver, small intestine, heart, and aorta and, to a lesser extent in the brain (31, 32). TASK2 is abundant in the kidney, salivary glands, colon, and immune T cells. In the brain, TASK2 expression is restricted to specific regions, such as brainstem nuclei, hippocampus, and cerebellum (33–36).

Here, we reexamine the coexpression of TALK1, TALK2, and TASK2 at the single-cell level and provide evidence of a physical and functional interaction between these subunits. Their heteromerization produces channels with unique pH sensitivity and single-channel properties.

## Results

### *TALK1, TALK2, and TASK2 subunits are coexpressed in tissues and cells*

In the previous studies reporting the identification and characterization of the TALK1, TALK2, and TASK2 channels, their tissue distribution was analyzed by Northern blots or RT–PCR (4, 5, 8, 30–36). These results cannot be used for comparing their relative expression levels in the tissues in which they are expressed, as the experimental conditions (blots and probes for Northern blot analysis, and complementary DNA [cDNA] templates and number of cycles for

PCR) were not the same. We reexamined the distribution of these channels by taking advantage of data collected using transcriptomics that allow such a comparison, in not only tissues but also in cells.

We first analyzed the expression of TALK1, TALK2, and TASK2 in the EMBL expression atlas database (https://www.ebi.ac.uk/gxa/). The analysis of an RNA-Seq dataset of 53 human tissues from the Genotype-Tissue Expression project shows that TASK2 and TALK2 are present in most tissues, whereas TALK1 has a more restricted distribution in pancreas, stomach, testis, and thyroid gland (Fig. 1*B*). Some tissues preferentially express one channel, such as TALK2 in aorta and coronary artery or TASK2 in the liver, ovary, colon, and bladder. In the lung, TALK2 and TASK2 are expressed at the same level. Only the pancreas expresses significant levels of the three channels (Fig. 1*B*).

Because tissues are composed of different cell types that have the potential to express these channels at different levels, we next analyzed their expression in the major cell types of the pancreas. Data were extracted from a previous RNA-Seq study that profiled human pancreatic cells using single-cell transcriptomics (37). We analyzed channel expression in endocrine (α, β, γ, δ, and ε) and exocrine (acinar and ductal) cells (Fig. 1*C*). All cell types express TALK1, TALK2, and TASK2. However, TASK2 was found to be less expressed, relative to TALK1 and TALK2 expression, than expected from the EMBL expression atlas database (Fig. 1*B*). This may be due to the expression of TASK2 in another pancreatic cell type or to interindividual variations between the samples analyzed in these two studies (variations related to age, gender, or ethnicity).

Because RNA-Seq was performed at the single-cell level (37), we were then able to analyze channel expression in individual cells of a given cell type. Figure 1*D* shows the analysis carried out for insulin-secreting β-cells. TALK1 was detected in 80 of the 99 cells studied (Fig. 1*D*). TALK2 was detected in 48 cells and TASK2 in 16 cells. Interestingly, both TALK1 and TALK2 were detected in 40 cells and TALK1 and TASK2 in three cells. TALK1, TALK2, and TASK2 were codetected in one cell of 99 analyzed.

Taken together, these results show that TALK1, TALK2, and TASK2 have overlapping tissue distribution, and that they can be coexpressed at the cell level in the pancreatic β-cells. This suggested, by inference with what we have previously shown for the TREK and THIK subfamilies, that TALK1, TALK2, and TASK2 could associate to form heterodimers.

### *TALK subunits physically interact in mammalian cells*

A physical interaction between TALK1, TALK2, and TASK2 was first tested using *in situ* proximity ligation assay (PLA) in cultured mammalian cells (Fig. 2*A*). This technique uses primary antibodies that bind to tags present on channel subunits.

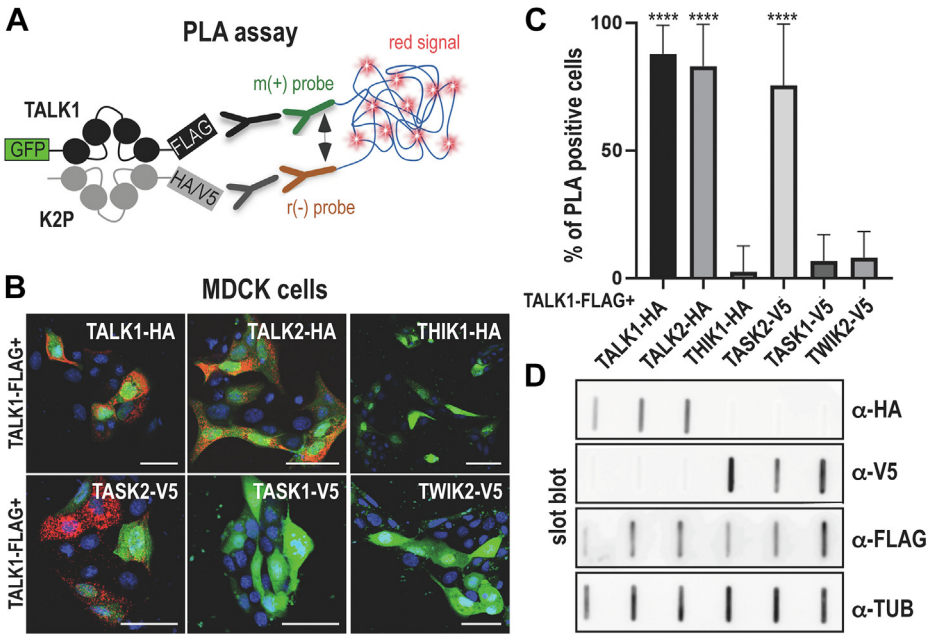


**Figure 2. Physical interaction of TALK1, TALK2, and TASK2 by proximity ligation assay (PLA) on tagged $K_{2P}$ channels expressed in MDCK cells.** *A*, schematic description. Cells were cotransfected with different combinations of TALK1-FLAG with various $K_{2P}$ subunits tagged with HA or V5. TALK1-FLAG was subcloned into pIRES2-EGFP to visualize transfected cells in *green*. Anti-TAG antibodies are specifically recognized by PLA complementary probes mouse PLUS (m+) and rabbit MINUS (r−). When the two PLA probes are close enough (<40 nm), a ligation generates circular DNA. This DNA is then amplified by a polymerase, and complementary fluorescent nucleotides are incorporated giving a *red* positive PLA signal. *B*, representative wide-field microscopy images. The scale bars represents 50 μm. *C*, quantification of the PLA signal. Percentage of cells is the number of PLA-positive cells (*red*) relative to the total number of transfected cells (*green*) from at least three independent experiments. Data represent means ± SD and were analyzed with Dunn's multiple comparison post hoc test for Kruskal–Wallis analysis. ****$p < 0.0001$ is obtained for TALK1-HA or TALK2-HA or TASK2-V5 *versus* THIK1-HA, TASK1-V5, and TWIK2-V5. *D*, slot blot analysis showing $K_{2P}$ subunit expression in MDCK cells. Cells were cotransfected in the same conditions as for PLA assay, and protein extracts were made and analyzed for $K_{2P}$ subunit expression with anti-TAG and antitubulin (TUB) antibodies. EGFP, enhanced GFP; HA, hemagglutinin; $K_{2P}$, two-pore domain potassium; MDCK, Madin–Darby canine kidney cell; PLA, proximity ligation assay; TALK1, TWIK1-related alkalinization-activated $K^+$ channel 1; TALK2, TWIK1-related alkalinization-activated $K^+$ channel 2; TASK2, TWIK1-related acid-sensitive $K^+$ channel 2; THIK1, TWIK1-related halothane-inhibited $K^+$ channel 1; TWIK2, tandem of p domains in a weak inward rectifying $K^+$ channel 2.

Primary antibodies are labeled with secondary antibodies containing cDNA strands. When antibodies are in close proximity (30–40 nm apart), the two strands hybridize, enabling subsequent DNA amplification by PCR. This amplification product is detected as a red fluorescent signal. Each pair of primary antibodies was tested for specificity (Fig. 2*B*). TALK1-FLAG subunit, cloned into the pIRES-enhanced GFP (EGFP) vector for green fluorescence coexpression, was expressed with TALK1-hemagglutinin (HA) or TALK1-V5 for positive controls (formation of homodimers). The percentage of positive cells was calculated by determining the ratio of cells with a positive signal (*red*) among the hundreds of transfected cells (*green*), from three to seven independent experiments (Fig. 2*C*).

Most cells showed a positive PLA signal when the TALK1 homodimer is formed, that is between TALK1-FLAG and TALK1-HA (88%). Similar values were obtained when TALK1-FLAG was expressed with TALK2-HA (83%) or TASK2-V5 (75%), whereas only 3, 7, and 8% of positive cells were obtained with THIK1-HA, TASK1-V5, and TWIK2-V5, respectively (Fig. 2*C*). A slot blot was performed on cell lysates under the same conditions as in the PLA experiments. Some differences in the expression level of the different $K_{2P}$ subunits are observed (Fig. 2*D*) but with no correlation with the results obtained in PLA. For example, TALK1-HA is less expressed than TALK2-HA and THIK1-HA, but the PLA signal is significantly higher with TALK1 and TALK2 than with THIK1 (Fig. 2*D*). These results show that TALK1 can form heterodimers with TALK2 and TASK2 but not with THIK1, a member of another $K_{2P}$ channel subfamily.

### *A dominant negative TALK1 subunit decreases TALK2 and TASK2 currents in* Xenopus *oocytes*

To confirm the interaction between TALK1, TALK2, and TASK2, we used a functional method based on channel poisoning with a nonfunctional subunit in *Xenopus* oocytes (Fig. 3*A*). The same DN strategy was used to demonstrate heteromerization in TREK and THIK $K_{2P}$ channel subfamilies (20, 21). In TALK1, we replaced the glycine residue at position 110 with a glutamate residue (G110E). This mutation in the pore domain of the channel leads to a loss of function. As expected, TALK1-G110E produced no measurable current (0.4 μA ± 0.1 *versus* 2.2 μA ± 0.3 for TALK1, at +60 mV, n = 9). To test its effect on TALK1, TALK1-G110E and TALK1 circular RNAs (cRNAs) were injected in equal amount. Representative current traces (Fig. 3*C*) and normalized mean current amplitudes (Fig. 3*B*) show that TALK1 is largely inhibited by TALK1-G110E (0.4 μA ± 0.1, n = 14) confirming the DN action of TALK1-G110E, renamed $TALK1^{DN}$.

We next coexpressed $TALK1^{DN}$ with other $K_{2P}$ subunits. In oocytes, expression of TALK2, TASK2, and THIK1 produced currents as expected (Fig. 3*C*). At +60 mV, the mean current amplitudes were 3.6 μA ± 0.7 (n = 12), 3.6 μA ± 1.7 (n = 16), and 4.6 μA ± 1.6 (n = 17), respectively. Coexpression of $TALK1^{DN}$ with TALK2 and TASK2 caused a dramatic decrease in current amplitude (Fig. 3*C*). The decrease reached 95% for TALK2 and 70% for TASK2, values that are comparable to the effect on TALK1 (60%). The decreases in TALK2 and TASK2 currents are consistent with the 75% decrease expected for a 1:1 ratio between DN and functional subunits (Fig. 3*A*). The smaller effect of $TALK1^{DN}$ on TALK1 (60%) is likely because of the fact that the baseline current of TALK1 is lower than that of TASK2 or TALK2 (∼1 μA for TALK1 *versus* ∼4 μA for TALK2 and TASK2) and that the current decrease cannot occur above endogenous oocyte current levels (∼100–300 nA). The inhibition of THIK1 by $TALK1^{DN}$ is much more limited (15%), suggesting a competitive effect on protein expression rather than heteromerization (Fig. 3, *B* and *C*). To ensure that the DN inhibition was by assembly and not due by a decrease in protein synthesis, the expression levels of the channels were determined by slot blot using the tags present on the different subunits (Fig. 3*B*). Thus, we found no major difference in channel or tubulin expression in the presence of $TALK1^{DN}$ under the different conditions. Taken together, the results of this electrophysiological approach confirm the formation of heteromers between TALK1 and TALK2 or TASK2.

### *TALK heterodimers exhibits unique pH sensitivity*

We then asked whether heteromerization between TALK1 and TALK2 or TASK2 produces heteromeric channels with distinct properties. An important characteristic of these channels is their sensibility to the extracellular pH. They are stimulated by alkalinization in the range of pH 7.5 to 10 (4, 5, 38). This sensitivity involves a pH sensor containing a titratable residue located in the extracellular P2-M4 loop: R242 in TALK1, K242 in TALK2, and R224 in TASK2 (39–41) (Fig. 4*A*). The substitution of this basic residue by a neutral residue confers insensitivity to alkalinization. To compare the pH sensitivity of TALK1, TALK2, and TASK2 under the same experimental conditions, they were expressed in *Xenopus* oocytes. The currents were measured at 0 mV, normalized to the currents measured at pH 10, and plotted as a function of the extracellular pH (Fig. 4*B*). As previously reported, each homodimeric channel has a unique profile of sensitivity to external pH, which is different from each other and from other pH-sensitive $K_{2P}$ channels including TASK and TREK channels (38). TALK1 is open above pH 6 with a biphasic pH-dependence curve (4, 41). pH-dependence curve for TASK2 is shifted to more alkaline values from pH 6 to 8 but then almost superpose with TALK1 second phase from pH 8 to 10 (Fig. 4*B*). The estimated $pK_{1/2}$ for the effect of pH on TASK2 is near 8, close to the values reported in mammalian cells (5, 41, 42). The pH dependence of TALK2 is significantly different from that of TALK1 and TASK2, with a shift to more alkaline values. As previously reported for this channel, almost no current is detected at physiological pH, then the current starts to increase sharply from pH 8 without apparent saturation at pH 10 (4) (Fig. 4*B*).

To study the pH sensibility of heterodimeric channels, we designed cDNAs for the expression of tandem chimeras in which two different subunits are covalently linked through the C terminus of the first subunit and the N terminus of the second subunit. This method allows access to currents produced by pure heterodimeric channels rather than by a

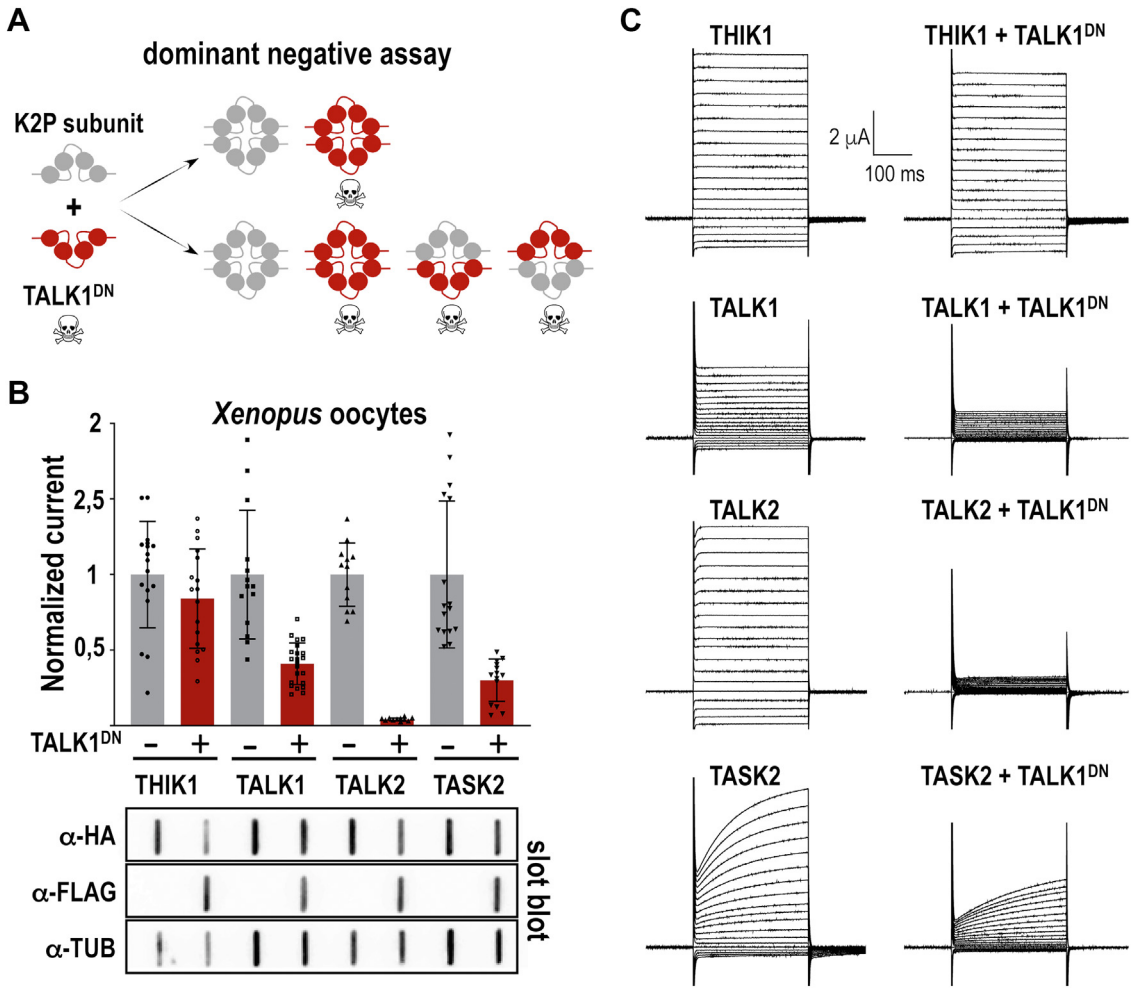


**Figure 3. Heterodimerization of TALK1, TALK2 and TASK2 shown by current inhibition by a dominant negative TALK1 (TALK1$^{DN}$) coexpressed in *Xenopus* oocytes.** *A*, method: a nonfunctional subunit (*red*) bearing a mutation in the pore domain (G110E) is coinjected in a 1:1 ratio with a functional $K_{2P}$ subunit. In the absence of heterodimerization, the current is not affected by TALK1$^{DN}$. If TALK1$^{DN}$ and the coexpressed subunit associate, then the heterodimers are nonfunctional and the current decreases by at least 75%. *B*, normalized steady-state average current amplitude at 0 mV current for oocytes expressing $K_{2P}$ subunit alone (–) or with (+) TALK1$^{DN}$, as shown. Data represent means ± SD and were analyzed with Dunn's multiple comparison test: ****$p < 0.0001$ is obtained for TALK2 *versus* TALK2 + TALK1$^{DN}$, ***$p < 0.001$ for TALK1 *versus* TALK1 + TALK1$^{DN}$, **$p < 0.01$ for TASK2 *versus* TASK2 + TALK1$^{DN}$, no significance for THIK1 *versus* THIK1 + TALK1$^{DN}$. *Lower panel*, slot blot analysis showing $K_{2P}$ subunit expression in *Xenopus* oocytes. TALK1, TALK2, TASK2, and THIK1 are HA tagged, and TALK1$^{DN}$ is tagged with FLAG. Tubulin (TUB) is used as a loading control. *C*, representative traces obtained from oocytes expressing TALK1, TALK2, TASK2, and THIK1 in the absence or the presence of TALK1$^{DN}$. Currents were recorded at membrane potentials ranging from −120 mV to +60 mV from a holding potential of −80 mV in 10 mV increments. TALK1, TWIK1-related alkalinization-activated $K^+$ channel 1; TALK2, TWIK1-related alkalinization-activated $K^+$ channel 2; TASK2, TWIK1-related acid-sensitive $K^+$ channel 2; THIK1, TWIK1-related halothane-inhibited $K^+$ channel 1; HA, hemagglutinin; $K_{2P}$, two-pore domain potassium.

mixture of homodimers and heterodimers, as observed when the two subunits are expressed separately. For TASK1–TASK3 tandems, differences in electrophysiological behavior have been reported depending on the order of the two subunits in the chimeras (43). We therefore designed and expressed cDNAs for both Td-TALK1–TALK2 and Td-TALK2–TALK1 channels. For tandems containing TASK2, only Td-TASK2–TALK1 and Td-TASK2–TALK2 yielded measurable currents, as the tandems with the opposite orientation (Td-TALK1–TASK2 and Td-TALK2–TASK2) produced no current, suggesting that a physical constraint on the N terminus of TASK2 could alter channel assembly and folding or trafficking to the plasma membrane. The pH dependence of the functional tandems was compared with the pH dependence of the corresponding homomers (Fig. 4*C*). Td-TALK1–TALK2 and Td-TALK2–TALK1 show an intermediate pH dependence compared with TALK1 and TALK2. The heterodimeric channels are inhibited at acidic pH and activated at basic pH with a dependence curve resembling the monophasic one of TALK2 but shifted to more acidic values. As for TALK2, the current increase is not saturating even under very basic conditions (pH 10). For Td-TASK2–TALK1 and Td-TASK2–TALK2, the pH-dependence curves are very similar and overlap with the curve for TASK2 (Fig. 4*C*). Compared with TALK2 alone, the combination of TASK2 with TALK2 results in more current around physiological values.

These results show that heteromerization has a very significant effect on the extracellular pH sensitivity of the TALK–TASK2 channels: association of TALK1 with TALK2, or of one of these subunits with TASK2, produces heterodimeric channels that behave like TASK2.

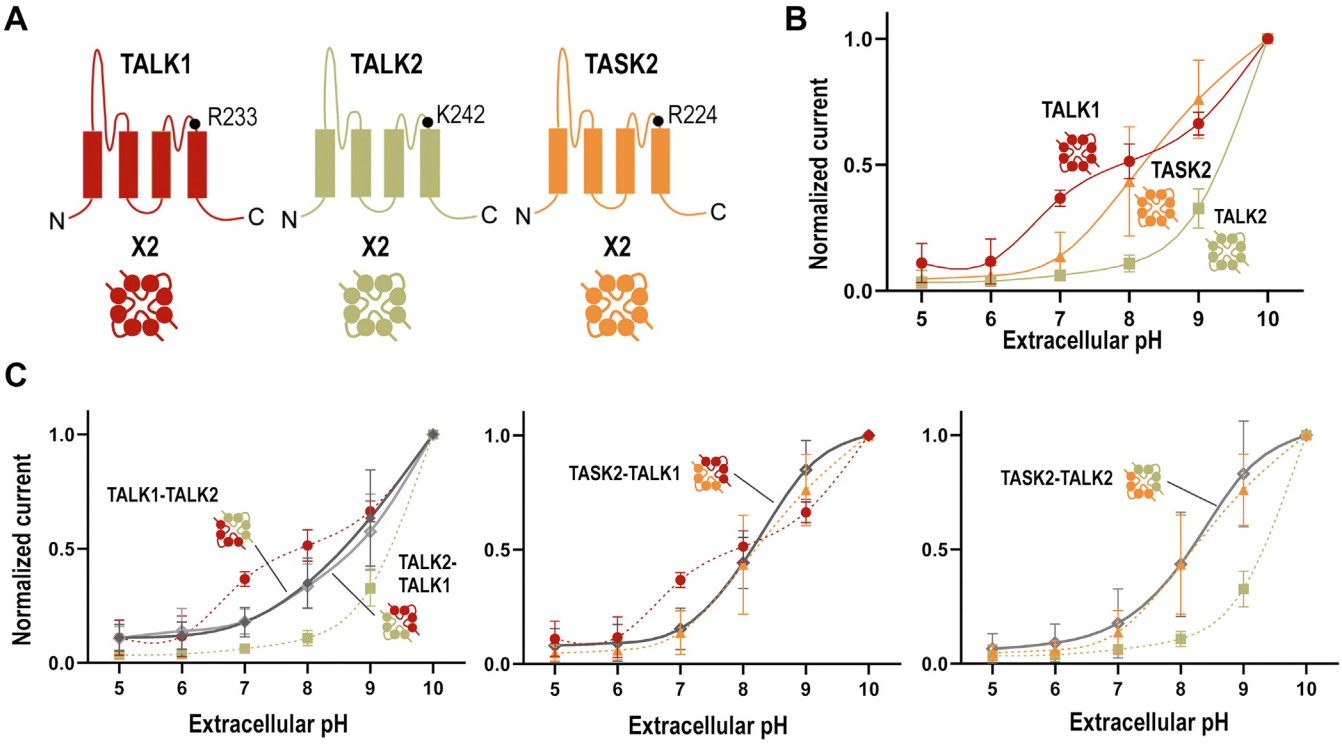


**Figure 4. Sensitivity to extracellular pH of homomeric and heteromeric TALK–TASK channels expressed in *Xenopus* oocytes.** *A*, overall topology of TALK–TASK2 subunits. Each subunit comprises four transmembrane domains, two extracellular pore regions, and cytoplasmic N terminus and C terminus. Basic residues involved in extracellular pH sensing are shown. *B* and *C*, pH-dependence curves measured with subunits expressed alone (*B*) or in covalently linked tandem (*C*). Values represent mean ± SD (n = 10–16) of currents measured at 0 mV, normalized to the currents measured at pH 10, and plotted against extracellular pH values. *C*, comparison of the extracellular pH-dependence curves. *Dashed lines* represent pH-dependence curves of homomeric channels as in (*B*). TALK, TWIK1-related alkalinization-activated $K^+$ channel; TASK, TWIK1-related acid-sensitive $K^+$ channel.

### *Single-channel properties of the TALK tandems*

We next compared the single-channel properties of homodimers and heterodimers in mammalian cells. Cell-attached patch recordings from human embryonic kidney 293 cells expressing TALK1, TALK2, and TASK2 show typical single-channel openings (Fig. 5). Under symmetric $K^+$ conditions (150 mM KCl, $pH_o$ = 7.4), TALK1 is active over the entire range of membrane potentials and shows very brief openings. The mean open time was less than 0.3 ms (0.2 ± 0.1 ms), close to reported values (30, 44) (Fig. 5*A*). The unitary conductance of TALK1 is 22 ± 1 pS at −80 mV and 9.8 ± 1 pS at +80 mV. The mean open time of TALK2 is 0.8 ± 0.1 ms (−80 mV), a value significantly higher than that of TALK1. The unitary conductance of TALK2 is 41 ± 3 pS at −80 mV and 14 ± 2 pS at +80 mV, values that are also significantly higher than those of TALK1 (Fig. 5*A*).

As observed in *Xenopus* oocytes (Fig. 4), Td-TALK1–TALK2 and Td-TALK2–TALK1 form functional channels in mammalian cells (Fig. 5*A*). They have unitary conductances of 12 ± 1 pS and ∼11 ± 1 pS at +80 mV and ∼23 ± 1 pS and ∼24 ± 3 pS at −80 mV, respectively. The tandems behave like TALK1. They have a linear current–voltage relationship, whereas TALK2 shows an inward rectification, producing more currents at −80 mV than at +80 mV. Unlike TALK1 and TALK2, TASK2 opened in long bursts containing many closing events within each burst (Fig. 5*B*). The mean open time of TASK2 is 2.0 ± 0.3 ms at −80 mV, and the unitary conductance is 32 ± 1 pS at +80 mV and 92 ± 7 pS at −80 mV. Td-TASK2–TALK1 and Td-TASK2–TALK2 have comparable unitary conductances to each other's and to TASK2, significantly different from TALK1 and TALK2. For all TASK2-containing channels, the current–voltage relations showed inward rectification.

These results show that heteromerization has a significant effect on single-channel properties of the TALK channels. Association of TALK1 with TALK2 produces heteromeric channels behaving more like TALK1, with lower unitary conductances and inward rectification, whereas association of TALK1 or TALK2 with TASK2 produces heterodimeric channels behaving more like TASK2 with higher unitary conductances and inward rectification.

### *Heteromerization of native TALK1 and TALK2 in human pancreatic β-cells*

The human pancreatic β-cell line, EndoC-βH5, is comparable to primary pancreatic cells. They express high levels of TALK1 and TALK2 (information given by the provider). These cells, like the native β-cells (Fig. 1*C*), express 100-fold lower amounts of TASK2. We therefore tested the hypothesis that endogenous TALK1 and TALK2 channels interact in EndoC-βH5 cells using the PLA method (Fig. 6*A*). The average number of puncta per cell was significantly higher when cells were incubated simultaneously with anti-TALK1 and anti-TALK2 antibodies rather than separately ($p < 0.001$,

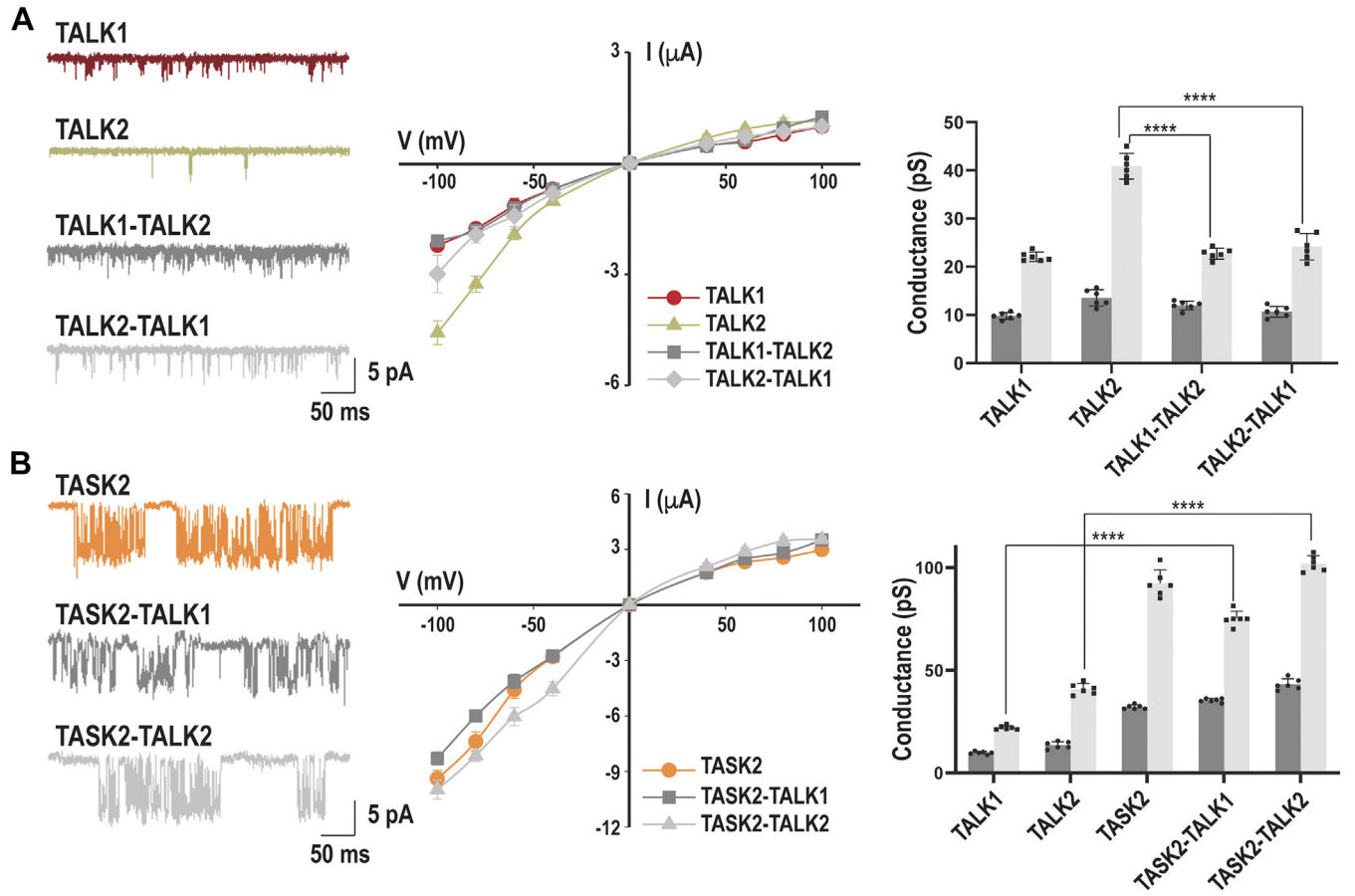


**Figure 5. Single-channel properties of homodimeric and heterodimeric channels in HEK293 cells.** *A* and *B*, single-channel recordings at −80 mV (*left panel*). Single-channel current–voltage relationships (n = 6) (*middle panel*). Currents were recorded in cell-attached patches held at pipette potentials from +100 mV to −100 mV in bath solution containing 150 mM KCl. Unitary conductances expressed as means ± SD at −80 and +80 mV (n = 6) (*right panel*). Data were analyzed by using two-way ANOVA and Tukey's multiple comparisons test: ****$p < 0.0001$. HEK293, human embryonic kidney 293 cell line.

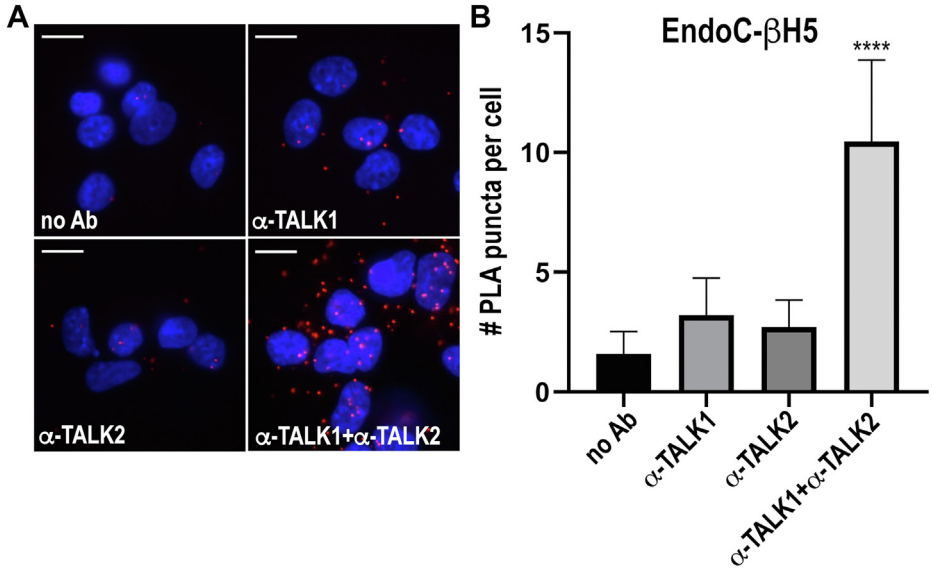


**Figure 6. Proximity ligation assay (PLC) in EndoC-βH5 cells.** *A*, representative images obtained with epifluorescence microscope (40×) of PLA signal from TALK1 and TALK2 heteromeric formation (*red puncta*) and associated negative controls. PLA was performed using anti-TALK1 mouse monoclonal and anti-TALK2 rabbit polyclonal primary antibodies and oligonucleotide-linked PLA secondary probes (mouse, m[+] and rabbit, r[−]). The scale bar represents 10 μm. Nucleus are shown in *blue* (DAPI). *B*, quantification of the average number of PLA-positive *red puncta* per cell for four independent experiments. Quantification was done using CellProfiler, and data were analyzed by two-way ANOVA using Tukey's multiple comparisons tests: ****$p < 0.0001$ α-TALK1 + α-TALK2 *versus* no Ab, *versus* α-TALK1 and *versus* α-TALK2. DAPI, 4′,6-diamidino-2-phenylindole; TALK1, TWIK1-related alkalinization-activated $K^+$ channel 1; TALK2, TWIK1-related alkalinization-activated $K^+$ channel 2.

Fig. 6*B*). Controls in which primary antibodies were omitted and PLA probes included show almost no puncta. These data support the conclusion that native TALK1 and TALK2 interact in human pancreatic β-cells.

## Discussion

A number of studies have focused on the heteromerization of $K_{2P}$ channels. These studies have produced interesting, but sometimes conflicting, results (for review, see Ref. (18)). Demonstrating that heteromerization occurs under native conditions is a major challenge. Several experimental conditions are unfavorable: the low level of endogenous expression of ion channels in general, and of background $K^+$ channels in particular, the absence of antibodies with affinity and selectivity allowing a specific immunolabeling of these channels, and also electrophysiological and pharmacological properties that make it difficult to distinguish between currents produced by homodimers and heterodimers. The prerequisite for heterodimer formation is the coexpression of two channel subunits not only in the same tissue but, more importantly, in the same cells of that tissue. The development of methods based on single-cell transcriptomics makes it possible to study such distribution. Among the tissues that coexpress TALK1, TALK2, and TASK2, we chose the pancreas to study their expression at the single-cell level. By analyzing data collected for another study, we show here that coexpression of two or three of the TALK1, TALK2, or TASK2 subunits can be detected in the same insulin-secreting β-cells (Fig. 1). Their ability to form heterodimers was next studied in heterologous expression systems (Figs. 2 and 3) and under native conditions in human pancreatic β-cells (Fig. 6). Two different methods were used: one based on immunolabeling of heterodimeric complexes in mammalian cells, and the second, more functional, on current poisoning using expression of a DN subunit in *Xenopus* oocytes. Both methods unambiguously showed that TALK1, TALK2, and TASK2 form heterodimers upon heterologous expression, and that native TALK1 and TALK2 form heterodimers in pancreatic cells. It should be noted that we did not observe the interaction between TALK2 and TASK1 that was previously reported (29). In their study, Suzuki *et al.* found that the TASK1 current was only partially inhibited by the coexpression of a DN of TALK2. Controls were missing such as the impact of the $TALK2^{DN}$ channel on other $K_{2P}$ channels or a dose-dependent inhibition of TASK1 by $TALK2^{DN}$. They did not confirm the potential interaction by another method.

Four splice variants of TALK1 were identified, but only two of them are functional (44). The two functional variants, TALK1a and TALK1b, differ in their cytoplasmic C terminus, but their electrophysiological characteristics are indistinguishable. In the variants TALK1c and TALK1d, the fourth transmembrane segment (M4) is missing. They do not induce current, and when coexpressed with TALK1a or TALK1b, they do not influence the current produced by these functional variants, suggesting that M4 is essential for correct folding and/or oligomerization. Because these isoforms of TALK1 lacking M4 do not interact with TALK1a and TALK1b, they are not expected to form heterodimers with TALK2 and TASK2.

A major function of heterodimerization is to increase channel diversity by producing channels with novel electrophysiological, pharmacological, or regulatory properties. Expression in *Xenopus* oocytes and mammalian cells has shown that this is the case for the TALK1, TALK2, and TASK2 heterodimers. TALK1–TALK2 channels show an intermediate sensitivity to extracellular pH, different from that of homodimeric TALK1 or TALK2 channels (Fig. 4). This suggests that each of the subunits transmits some of its properties to the heterodimer. TASK2–TALK1 and TASK2–TALK2 heterodimers have a similar sensitivity to external pH as TASK2. Recently, R233 in TALK1 has been identified as the primary pH sensor. This residue located at the N terminus of transmembrane segment 4 remotely regulates the orientation of the carbonyl group at the S1 potassium-binding site in the selectivity filter (SF), *via* a network composed of interacting residues on transmembrane segment 4, the pore helix domain 1, and the SF (45). This allosteric coupling between the pH sensor and SF regulates channel gating and may explain the hybrid pH sensitivity in TALK1–TALK2 heteromers as well as the lack of dominant effect in TALK1–TASK2 heteromers, with pH sensitivity not only dictated by pH sensor but also by the nature of those residues involved in the allosteric coupling. This is also observed with the single-channel properties (Fig. 5). Both in terms of unitary conductance and rectification, TASK2–TALK1 and TASK2–TALK2 are more similar to TASK2 than to TALK1 and TALK2. This implies that the TASK2 subunit is dominant over TALK1 or TALK2 in the TASK2–TALK1 and TASK2–TALK2 heterodimers.

External pH is not the only factor that regulates TALK channels. TALK2 is also regulated by intracellular pH by a mechanism independent of that described for external pH (39, 46). TALK channels have the highest level of expression in the duodenum and pancreas, where body fluids can be alkaline, suggesting that their sensitivity to alkalosis is physiologically relevant in these tissues. However, TALK2 is activated by alkaline pH outside the range encountered physiologically. Even in pancreatic ductal cells where the apical membrane is exposed to alkaline pancreatic juice (pH 8), only a very limited amount of the TALK2 homomeric channel would be open. The combination of TALK2 with TALK1 or with TASK2 could confer to these heterodimeric channels a pH sensitivity more compatible with extracellular pH variations in the physiological range.

Beside pH, a number of other mechanisms are involved in the regulation of these channels. Binding sites for Gβγ, $PIP_2$, phosphorylation, and 14-3-3 were also identified in the cytoplasmic C terminus of TASK2 (47–49). On the other hand, TALK1 and TALK2 channels are regulated by nitric oxide and reactive oxygen species such as superoxide ion ($O_2^-$) and singlet oxygen ($^1O_2$) (6). Intracellular osteopontin, a small proinflammatory molecule, specifically interacts with TALK1 and modulates its activity (50). Because the properties of the heterodimers cannot be inferred from the properties of the

corresponding homodimers, these regulations will need to be studied on heterodimers expressed in heterologous systems. A precise knowledge of these regulations is essential to study their functional contribution in native tissues.

A number of pathological mutations and polymorphisms have been identified in TALK1 and TALK2 that generate either more active channels or channels less active with DN properties (10–12). The impact of these mutations on heterodimers will also need to be studied. Finally, there is no specific pharmacology for TALK channels. Propanolol and propafenone, two beta-blockers with antiarrhythmic effects, have been shown to be responsible for a twofold to threefold activation of TALK2, but their effect on TALK1 and TALK2 has not been studied (51). Pyrazole derivatives, used for their analgesic properties, have also been tested on TASK2 but not on TALK channels (52). Lidocaine and bupivacaine, two local anesthetics, inhibit TASK2 (53). Although these molecules are not very specific for TASK2, they could possibly be tested on TASK2-containing heterodimeric channels provided that they are not or only slightly active on the other subunits of the heteromer (TALK1 or TALK2).

Since the ultimate goal of studying $K_{2P}$ heteromerization is to determine the physiological roles of heterodimers, we will need to identify specific pharmacological modulators and/or to design tools capable of disrupting endogenous heterodimers, to alter their function *in vivo*. Inducible mouse models expressing DN subunits such as $TALK1^{DN}$ would be useful to study the role of homodimer and heterodimers, for example, in endocrine and exocrine pancreatic cells and cardiomyocytes.

## Experimental procedures

### Constructs

Human TALK1, TALK2, and TASK2 coding sequences (Ensembl accession numbers: ENST00000373229.9, ENST 00000373231.9, and ENST00000359534.4) were inserted into pLIN, a modified pGEM vector for expression in *Xenopus* oocytes, and pcDNA3-Zeo (Invitrogen) for expression in mammalian cells. The cDNA coding $TALK1^{DN}$ was generated by site-directed mutagenesis using PCR and PfuTurbo DNA polymerase (Agilent). The whole cDNAs were sequenced. Tandems were constructed by overlapping PCRs and cloned into pLIN and pcDNA3-Zeo. For immunocytochemistry experiments, HA (YPYDVPDYA), FLAG (DYKDDDDK), or V5 (GKPIPNPLLGLDST) tags were inserted at the C terminus of the subunits. For *in situ* PLA and single-channel recordings, sequences encoding TALK1, TALK2, TASK2, Td-TALK1–TALK2, Td-TALK2–TALK1, Td-TASK2–TALK1, and Td-TASK2–TALK2 were subcloned into the pIRES2-EGFP vector (Invitrogen).

### Transfection and PLA of Madin–Darby canine kidney cells

Madin–Darby canine kidney (MDCK) cells are particularly well suited for *in situ* PLA assay because of their high transfection efficiency and because they adhere perfectly to the glass without precoating, which considerably limits cell loss during the many PLA steps. Cells, grown on coverslips in 24-well plates, were transiently transfected with DNA plasmids (0.5 μg each). Cells were fixed, permeabilized, and incubated with primary mouse anti-FLAG (M2; Sigma, 1/1000 dilution) and rabbit anti-HA (Santacruz Ab; catalog no.: sc-805, 1/1000 dilution) or rabbit anti-V5 (PRB-189P; Covance, 1/1000 dilution) antibodies for 2 h at 37 °C in antibody diluent solution (Duolink *in situ* kit; Sigma–Aldrich). The cells were then labeled with the PLA antimouse PLUS probe (DUO92001) and the PLA anti-rabbit MINUS probe (DUO92005) purchased from Sigma–Aldrich. Detection was performed with Duolink *in situ* detection reagents red kit (DUO92008) according to the manufacturer's protocol. Finally, the coverslips were mounted on slides, and the fields were imaged randomly using a Zeiss microscope with a 40× objective with appropriate filters for the detection fluorophore used (Texas Red, eGFP, and 4′,6-diamidino-2-phenylindole). Images were acquired in one plane, and the same settings (exposure time and gain) were used to capture all images within an experiment (10 fields per condition and per experiment). Because of the overexpression, the PLA signals merge within the cells and the image pixels are saturated. For this reason, the image data are analyzed for the percentage of PLA-positive cells (*red cells*) compared with the number of transfected cells (*green cells*). Differences between groups were analyzed using Dunn's multiple comparison post hoc test for Kruskal–Wallis analysis. The significance level was set at $p < 0.0001$. Data were represented as mean ± SD.

### Oocyte expression and two-electrode voltage clamp recordings

Capped cRNAs were synthesized using the AmpliCap-Max T7 high yield message maker kit (CellScript) from plasmids linearized by AflII. RNA concentration was quantified using a NanoDrop (Thermo Fisher Scientific). *Xenopus laevis* stage V–VI oocytes were injected with 20 ng of each cRNA and maintained at 18 °C in ND96 solution (96 mM NaCl, 2 mM KCl, 2 mM $MgCl_2$, 1.8 mM $CaCl_2$, 5 mM Hepes, pH 7.4 adjusted with NaOH). Oocytes were used 1 to 2 days after injection. Macroscopic currents were recorded with a two-electrode voltage clamp (Dagan TEV 200). The electrodes were filled with 3 M KCl and had a resistance of 0.5 to 2 MΩ. A small chamber with a fast perfusion system was used to change extracellular solutions and was connected to the ground with a 3 M KCl-agarose bridge. All currents were recorded in ND96 at different pH value from 5 to 10 adjusted with NaOH. For pH <6, the solution was buffered with 5 mM Mes, and for pH >9, the solution was buffered with 5 mM Tris. Currents were evoked by 300 ms steps by voltage pulses ranging from −120 mV to +60 mV in 10 mV steps from a holding potential of −80 mV. Stimulation of the preparation, data acquisition, and analysis were performed using pClamp software (Molecular Devices). All recordings were performed at 20 °C.

### Slot blots from MDCK cells and oocytes

MDCK cells, grown in 35 mm dishes, were transiently transfected with DNA plasmids (2 μg each). About 24 h after transfection, cells were lysed in 500 μl of a lysis buffer (PBS: 40% [w/w] glycerol, 2% [w/w] CHAPS, 140 mM NaCl, 2 mM EDTA,

20 mM Tris, pH 8.8, supplemented with protease inhibitor mixture). For protein expressed in oocytes, extraction was done by pipetting up and down in 10 μl/oocyte of the same lysis buffer. MDCK and oocyte's lysates were centrifuged at 20,800*g* for 30 min at 4 °C, the supernatant was combined with Laemmli loading buffer, and blotted onto a nitrocellulose membrane. The membranes were probed with anti-HA (Santacruz Ab; catalog no.: sc-805, 1/1000 dilution), anti-V5 (PRB-189P; Covance, 1/1000 dilution), anti-FLAG (M2; Sigma, 1/1000 dilution), anti–β-tubulin (Sigma–Aldrich; catalog no.: T8453, 1/1000 dilution) antibodies, and horseradish peroxidase–coupled secondary antibodies (Jackson ImmunoResearch; 1/10,000 dilution). Chemiluminescent signals were analyzed with a Fusion FX imaging system (Vilber).

### Single-channel recording

Human embryonic kidney 293 cells were transfected with pIRES2-EGFP plasmids containing the coding sequences of TALK1, TALK2, TASK2, Td-TALK1–TALK2, Td-TALK2–TALK1, Td-TASK2–TALK1, and Td-TASK2–TALK2 using Lipofectamine 2000 and Opti-MEM medium (Life Technologies). The cells were used 2 days after transfection. Electrophysiological recording was performed using a patch clamp amplifier (Axopatch 200B; Molecular Devices). Glass patch pipettes (thick-walled borosilicate; Warner Instruments) coated with SYLGARD were used to minimize background noise. The currents were filtered at 2 kHz and transferred to a computer using the Digidata 1320 interface at a sampling rate of 20 kHz. Single-channel currents were analyzed with the pClamp program, and the plots shown in the figures were filtered at 2 kHz. For single-channel current analysis, the amplitude of each channel was set to 0.53 pA, and the minimum duration was set to 0.05 ms. In experiments using cell-attached patches, pipette and bath solutions contained (in millimolar): 150 KCl, 1 $MgCl_2$, 5 EGTA, 10 glucose, and 10 Hepes (pH 7.3). All experiments were performed at 25 °C. Differences among groups were analyzed using a two-way ANOVA and a Tukey's multiple comparison test. The significance level was set at $p < 0.0001$. Data were represented as mean ± SD.

### EndoC-βH5 cells and Duolink PLA

A 1 ml cryovial containing 5 million cryopreserved EndoC-βH5 cells was thawed, and the cells were seeded in five different well plates in the complete culture medium provided by the manufacturer (ULTIβ1; Human Cell Design). Four wells per 24-well plate, containing coated coverslips (β coat; Human Cell Design) were prepared containing each 200,000 cells. Each plate was used in an independent PLA experiment. Cells were fixed 10 min in paraformaldehyde 4%, permeabilized for 30 min with PBS containing 0.1% Triton X-100, and incubated 30 min in blocking solution from Duolink *in situ* kit. Cells were then incubated with mouse anti-TALK1 (Millipore; catalog no.: MABN2408, 1/100 dilution) and rabbit anti-TALK2 (Merck; catalog no.: HAP043892, 1/1000 dilution) overnight at 4 °C in antibody diluent solution. Cells were then labeled with the PLA antimouse PLUS probe (DUO92001) and the PLA anti-rabbit MINUS probe (DUO92005) purchased from Sigma–Aldrich. Detection was performed with Duolink *in situ* detection reagent red kit (DUO92008) according to the manufacturer's protocol. The coverslips were mounted on slides, and the fields were imaged randomly using a Zeiss microscope with a 40× objective, with the appropriate filters for the detection of the fluorophores (Texas Red and 4′,6-diamidino-2-phenylindole). Images were acquired in one plane, and the same settings were used to capture all images within an experiment (15 fields per condition and per experiment). The PLA signal was quantified using CellProfiler software (https://cellprofiler.org/) by automatically counting the total number of PLA puncta and the number of nuclei for each field (about 1500–2500 cells were counted in total). Differences among groups were analyzed using Dunn's multiple comparison post hoc test for Kruskal–Wallis analysis. The significance level was set at $p < 0.0001$. Data were represented as mean ± SD.

## Data availability

All data are contained within the article. Any additional information required to reanalyze the data reported in this article is available from the corresponding author upon request (lesage@ipmc.cnrs.fr).

*Acknowledgments*—We thank Martine Jodar and Marie-Emmanuelle Kerros for excellent technical assistance in molecular biology, Roberta Chiavetta, Charlotte Montillot, and Juliette Soubra for their help on this project during their internship, Nathalie Leroudier for assistance in sequencing analysis, and Frederic Brau for support in microscopy. This work was funded by the Agence Nationale de la Recherche (Laboratory of Excellence "Ion Channel Science and Therapeutics," grant ANR-11-LABX-0015-01) and the Fondation pour la Recherche Médicale (équipe labelisée FRM 2020).

*Author contributions*—L. K., N. G., E.-J. K., F. C. C., S. F., S. A., D. K., and D. B. investigation; D. K., F. L., and D. B. writing–review & editing.

*Funding and additional information*—This work was funded by the Ministry of Education (NRF-2021R1I1A3044128) to D. K.

*Conflict of interest*—The authors declare that they have no conflicts of interest with the contents of this article.

*Abbreviations*—The abbreviations used are: cDNA, complementary DNA; cRNA, circular RNA; DN, dominant negative; EGFP, enhanced GFP; GSIS, glucose-stimulated insulin secretion; HA, hemagglutinin; $K_{2P}$, two-pore domain potassium; MDCK, Madin–Darby canine kidney cell; PLA, proximity ligation assay; SF, selectivity filter; TALK1, TWIK1-related alkalinization-activated $K^+$ channel 1; TALK2, TWIK1-related alkalinization-activated $K^+$ channel 2; TASK, TWIK1-related acid-sensitive $K^+$ channel.

## References

1. Feliciangeli, S., Chatelain, F. C., Bichet, D., and Lesage, F. (2015) The family of K2P channels: salient structural and functional properties. *J. Physiol.* **593**, 2587–2603

2. Niemeyer, M. I., Cid, L. P., Gonzalez, W., and Sepulveda, F. V. (2016) Gating, regulation, and structure in K2P K+ channels: in varietate Concordia? *Mol. Pharmacol.* **90**, 309–317
3. Renigunta, V., Schlichthorl, G., and Daut, J. (2015) Much more than a leak: structure and function of K(2)p-channels. *Pflugers Arch.* **467**, 867–894
4. Girard, C., Duprat, F., Terrenoire, C., Tinel, N., Fosset, M., Romey, G., *et al.* (2001) Genomic and functional characteristics of novel human pancreatic 2P domain K(+) channels. *Biochem. Biophys. Res. Commun.* **282**, 249–256
5. Reyes, R., Duprat, F., Lesage, F., Fink, M., Salinas, M., Farman, N., *et al.* (1998) Cloning and expression of a novel pH-sensitive two pore domain K+ channel from human kidney. *J. Biol. Chem.* **273**, 30863–30869
6. Duprat, F., Girard, C., Jarretou, G., and Lazdunski, M. (2005) Pancreatic two P domain K+ channels TALK-1 and TALK-2 are activated by nitric oxide and reactive oxygen species. *J. Physiol.* **562**, 235–244
7. Vierra, N. C., Dadi, P. K., Jeong, I., Dickerson, M., Powell, D. R., and Jacobson, D. A. (2015) Type 2 diabetes-associated K+ channel TALK-1 modulates beta-cell electrical excitability, second-phase insulin secretion, and glucose homeostasis. *Diabetes* **64**, 3818–3828
8. Vierra, N. C., Dadi, P. K., Milian, S. C., Dickerson, M. T., Jordan, K. L., Gilon, P., *et al.* (2017) TALK-1 channels control beta cell endoplasmic reticulum Ca(2+) homeostasis. *Sci. Signal.* **10**, eaan2883
9. Cho, Y. S., Lee, J. Y., Park, K. S., and Nho, C. W. (2012) Genetics of type 2 diabetes in East Asian populations. *Curr. Diab. Rep.* **12**, 686–696
10. Mahajan, R., and Gupta, K. (2014) Prevention and management of type 2 diabetes: potential role of genomics. *Int. J. Appl. Basic Med. Res.* **4**, S1
11. Graff, S. M., Johnson, S. R., Leo, P. J., Dadi, P. K., Dickerson, M. T., Nakhe, A. Y., *et al.* (2021) A KCNK16 mutation causing TALK-1 gain of function is associated with maturity-onset diabetes of the young. *JCI Insight* **6**, e138057
12. Friedrich, C., Rinne, S., Zumhagen, S., Kiper, A. K., Silbernagel, N., Netter, M. F., *et al.* (2014) Gain-of-function mutation in TASK-4 channels and severe cardiac conduction disorder. *EMBO Mol. Med.* **6**, 937–951
13. Gestreau, C., Heitzmann, D., Thomas, J., Dubreuil, V., Bandulik, S., Reichold, M., *et al.* (2010) Task2 potassium channels set central respiratory CO2 and O2 sensitivity. *Proc. Natl. Acad. Sci. U. S. A.* **107**, 2325–2330
14. Barriere, H., Belfodil, R., Rubera, I., Tauc, M., Lesage, F., Poujeol, C., *et al.* (2003) Role of TASK2 potassium channels regarding volume regulation in primary cultures of mouse proximal tubules. *J. Gen. Physiol.* **122**, 177–190
15. Warth, R., Barriere, H., Meneton, P., Bloch, M., Thomas, J., Tauc, M., *et al.* (2004) Proximal renal tubular acidosis in TASK2 K+ channel-deficient mice reveals a mechanism for stabilizing bicarbonate transport. *Proc. Natl. Acad. Sci. U. S. A.* **101**, 8215–8220
16. Reed, A. P., Bucci, G., Abd-Wahab, F., and Tucker, S. J. (2016) Dominant-negative effect of a missense variant in the TASK-2 (KCNK5) K+ channel associated with balkan endemic nephropathy. *PLoS One* **11**, e0156456
17. Toncheva, D., Mihailova-Hristova, M., Vazharova, R., Staneva, R., Karachanak, S., Dimitrov, P., *et al.* (2014) NGS nominated CELA1, HSPG2, and KCNK5 as candidate genes for predisposition to Balkan endemic nephropathy. *Biomed. Res. Int.* **2014**, 920723
18. Khoubza, L., Chatelain, F. C., Feliciangeli, S., Lesage, F., and Bichet, D. (2021) Physiological roles of heteromerization: focus on the two-pore domain potassium channels. *J. Physiol.* **599**, 1041–1055
19. Czirjak, G., and Enyedi, P. (2002) Formation of functional heterodimers between the TASK-1 and TASK-3 two-pore domain potassium channel subunits. *J. Biol. Chem.* **277**, 5426–5432
20. Blin, S., Ben Soussia, I., Kim, E. J., Brau, F., Kang, D., Lesage, F., *et al.* (2016) Mixing and matching TREK/TRAAK subunits generate heterodimeric K2P channels with unique properties. *Proc. Natl. Acad. Sci. U. S. A.* **113**, 4200–4205
21. Blin, S., Chatelain, F. C., Feliciangeli, S., Kang, D., Lesage, F., and Bichet, D. (2014) Tandem pore domain halothane-inhibited K+ channel subunits THIK1 and THIK2 assemble and form active channels. *J. Biol. Chem.* **289**, 28202–28212
22. Lengyel, M., Czirjak, G., and Enyedi, P. (2016) Formation of functional heterodimers by TREK-1 and TREK-2 two-pore domain potassium channel subunits. *J. Biol. Chem.* **291**, 13649–13661
23. Levitz, J., Royal, P., Comoglio, Y., Wdziekonski, B., Schaub, S., Clemens, D. M., *et al.* (2016) Heterodimerization within the TREK channel subfamily produces a diverse family of highly regulated potassium channels. *Proc. Natl. Acad. Sci. U. S. A.* **113**, 4194–4199
24. Choi, J. H., Yarishkin, O., Kim, E., Bae, Y., Kim, A., Kim, S. C., *et al.* (2018) TWIK-1/TASK-3 heterodimeric channels contribute to the neurotensin-mediated excitation of hippocampal dentate gyrus granule cells. *Exp. Mol. Med.* **50**, 1–13
25. Hwang, E. M., Kim, E., Yarishkin, O., Woo, D. H., Han, K. S., Park, N., *et al.* (2014) A disulphide-linked heterodimer of TWIK-1 and TREK-1 mediates passive conductance in astrocytes. *Nat. Commun.* **5**, 3227
26. Lengyel, M., Czirjak, G., Jacobson, D. A., and Enyedi, P. (2020) TRESK and TREK-2 two-pore-domain potassium channel subunits form functional heterodimers in primary somatosensory neurons. *J. Biol. Chem.* **295**, 12408–12425
27. Plant, L. D., Zuniga, L., Araki, D., Marks, J. D., and Goldstein, S. A. (2012) SUMOylation silences heterodimeric TASK potassium channels containing K2P1 subunits in cerebellar granule neurons. *Sci. Signal.* **5**, ra84
28. Royal, P., Andres-Bilbe, A., Avalos Prado, P., Verkest, C., Wdziekonski, B., Schaub, S., *et al.* (2019) Migraine-associated TRESK mutations increase neuronal excitability through alternative translation initiation and inhibition of TREK. *Neuron* **101**, 232–245.e236
29. Suzuki, Y., Tsutsumi, K., Miyamoto, T., Yamamura, H., and Imaizumi, Y. (2017) Heterodimerization of two pore domain K+ channel TASK1 and TALK2 in living heterologous expression systems. *PLoS One* **12**, e0186252
30. Kang, D., and Kim, D. (2004) Single-channel properties and pH sensitivity of two-pore domain K+ channels of the TALK family. *Biochem. Biophys. Res. Commun.* **315**, 836–844
31. Decher, N., Maier, M., Dittrich, W., Gassenhuber, J., Bruggemann, A., Busch, A. E., *et al.* (2001) Characterization of TASK-4, a novel member of the pH-sensitive, two-pore domain potassium channel family. *FEBS Lett.* **492**, 84–89
32. Saez-Hernandez, L., Peral, B., Sanz, R., Gomez-Garre, P., Ramos, C., Ayuso, C., *et al.* (2003) Characterization of a 6p21 translocation breakpoint in a family with idiopathic generalized epilepsy. *Epilepsy Res.* **56**, 155–163
33. Cazals, Y., Bevengut, M., Zanella, S., Brocard, F., Barhanin, J., and Gestreau, C. (2015) KCNK5 channels mostly expressed in cochlear outer sulcus cells are indispensable for hearing. *Nat. Commun.* **6**, 8780
34. Gob, E., Bittner, S., Bobak, N., Kraft, P., Gobel, K., Langhauser, F., *et al.* (2015) The two-pore domain potassium channel KCNK5 deteriorates outcome in ischemic neurodegeneration. *Pflugers Arch.* **467**, 973–987
35. Shi, Y., Stornetta, R. L., Stornetta, D. S., Onengut-Gumuscu, S., Farber, E. A., Turner, S. D., *et al.* (2017) Neuromedin B expression defines the mouse retrotrapezoid nucleus. *J. Neurosci.* **37**, 11744–11757
36. Wang, S., Benamer, N., Zanella, S., Kumar, N. N., Shi, Y., Bevengut, M., *et al.* (2013) TASK-2 channels contribute to pH sensitivity of retrotrapezoid nucleus chemoreceptor neurons. *J. Neurosci.* **33**, 16033–16044
37. Segerstolpe, A., Palasantza, A., Eliasson, P., Andersson, E. M., Andreasson, A. C., Sun, X., *et al.* (2016) Single-cell transcriptome profiling of human pancreatic islets in health and type 2 diabetes. *Cell Metab.* **24**, 593–607
38. Lesage, F., and Barhanin, J. (2011) Molecular physiology of pH-sensitive background K(2P) channels. *Physiology (Bethesda)* **26**, 424–437
39. Li, B., Rietmeijer, R. A., and Brohawn, S. G. (2020) Structural basis for pH gating of the two-pore domain K(+) channel TASK2. *Nature* **586**, 457–462
40. Niemeyer, M. I., Gonzalez-Nilo, F. D., Zuniga, L., Gonzalez, W., Cid, L. P., and Sepulveda, F. V. (2006) Gating of two-pore domain K+ channels by extracellular pH. *Biochem. Soc. Trans.* **34**, 899–902
41. Niemeyer, M. I., Gonzalez-Nilo, F. D., Zuniga, L., Gonzalez, W., Cid, L. P., and Sepulveda, F. V. (2007) Neutralization of a single arginine residue gates open a two-pore domain, alkali-activated K+ channel. *Proc. Natl. Acad. Sci. U. S. A.* **104**, 666–671

42. Zuniga, L., Marquez, V., Gonzalez-Nilo, F. D., Chipot, C., Cid, L. P., Sepulveda, F. V., *et al.* (2011) Gating of a pH-sensitive K(2P) potassium channel by an electrostatic effect of basic sensor residues on the selectivity filter. *PLoS One* **6**, e16141
43. Rinne, S., Kiper, A. K., Schlichthorl, G., Dittmann, S., Netter, M. F., Limberg, S. H., *et al.* (2015) TASK-1 and TASK-3 may form heterodimers in human atrial cardiomyocytes. *J. Mol. Cell Cardiol.* **81**, 71–80
44. Han, J., Kang, D., and Kim, D. (2003) Functional properties of four splice variants of a human pancreatic tandem-pore K+ channel, TALK-1. *Am. J. Physiol. Cell Physiol.* **285**, C529–C538
45. Tsai, W. H., Grauffel, C., Huang, M. Y., Postic, S., Rupnik, M. S., Lim, C., *et al.* (2022) Allosteric coupling between transmembrane segment 4 and the selectivity filter of TALK1 potassium channels regulates their gating by extracellular pH. *J. Biol. Chem.* **298**, 101998
46. Niemeyer, M. I., Cid, L. P., Pena-Munzenmayer, G., and Sepulveda, F. V. (2010) Separate gating mechanisms mediate the regulation of K2P potassium channel TASK-2 by intra- and extracellular pH. *J. Biol. Chem.* **285**, 16467–16475
47. Anazco, C., Pena-Munzenmayer, G., Araya, C., Cid, L. P., Sepulveda, F. V., and Niemeyer, M. I. (2013) G protein modulation of K2P potassium channel TASK-2: a role of basic residues in the C terminus domain. *Pflugers Arch.* **465**, 1715–1726
48. Fernandez-Orth, J., Ehling, P., Ruck, T., Pankratz, S., Hofmann, M. S., Landgraf, P., *et al.* (2017) 14-3-3 Proteins regulate K2P 5.1 surface expression on T lymphocytes. *Traffic* **18**, 29–43
49. Niemeyer, M. I., Cid, L. P., Paulais, M., Teulon, J., and Sepulveda, F. V. (2017) Phosphatidylinositol (4,5)-bisphosphate dynamically regulates the K2P background K(+) channel TASK-2. *Sci. Rep.* **7**, 45407
50. Dickerson, M. T., Vierra, N. C., Milian, S. C., Dadi, P. K., and Jacobson, D. A. (2017) Osteopontin activates the diabetes-associated potassium channel TALK-1 in pancreatic beta-cells. *PLoS One* **12**, e0175069
51. Staudacher, I., Illg, C., Chai, S., Deschenes, I., Seehausen, S., Gramlich, D., *et al.* (2018) Cardiovascular pharmacology of K2P17.1 (TASK-4, TALK-2) two-pore-domain K(+) channels. *Naunyn Schmiedebergs Arch. Pharmacol.* **391**, 1119–1131
52. Kim, H. J., Woo, J., Nam, Y., Nam, J. H., and Kim, W. K. (2016) Differential modulation of TWIK-related K(+) channel (TREK) and TWIK-related acid-sensitive K(+) channel 2 (TASK2) activity by pyrazole compounds. *Eur. J. Pharmacol.* **791**, 686–695
53. Kindler, C. H., Paul, M., Zou, H., Liu, C., Winegar, B. D., Gray, A. T., *et al.* (2003) Amide local anesthetics potently inhibit the human tandem pore domain background K+ channel TASK-2 (KCNK5). *J. Pharmacol. Exp. Ther.* **306**, 84–92